



Contents lists available at ScienceDirect

Sensors & Actuators: B. Chemical

journal homepage: www.elsevier.com



Manipulation of fluid flow direction in microfluidic paper-based analytical devices with an ionogel negative passive pump

Tugce Akyazi^{a, b}, Nerea Gil-González^c, L. Basabe-Desmouts^{d, e}, E. Castaño^c, M.C. Morant-Miñana^f, Fernando Benito-Lopez^{a, g, *}

^a Analytical Microsystems & Materials for Lab-on-a-Chip (AMMa-LOAC) Group, Microfluidics Cluster UPV/EHU, Analytical Chemistry Department, University of the Basque Country UPV/EHU, Vitoria-Gasteiz, Spain

^b University of Navarra, TECNUN, Spain

^c CEIT and Tecnun (University of Navarra), Donostia-San Sebastián, Spain

^d BIOMICs microfluidics, Microfluidics Cluster UPV/EHU, Lascazar Ikerkunea Research Center, University of the Basque Country UPV/EHU, Vitoria-Gasteiz, Spain

^e Ikerbasque, Basque Foundation for Science, 48011 Bilbao, Spain

^f CIC nanoGUNE Consolider, Donostia-San Sebastián, Spain

^g Insight Centre for Data Analytics, National Centre for Sensor Research, Dublin City University, Dublin, Ireland

ARTICLE INFO

Article history:

Received 17 November 2016

Received in revised form 22 February 2017

Accepted 28 February 2017

Available online xxx

Keywords:

Ionogel

Passive pump

Microfluidic paper-based analytical device

Poly(*N*-isopropylacrylamide)

Ionic liquid

ABSTRACT

Microfluidic paper-based analytical devices (μ PADs) are a relatively new group of analytical tools that represent an innovative low-cost platform technology for fluid handling and analysis. Nonetheless, μ PADs lack in the effective handling and controlling of fluids, which leads to a main drawback for their reproducibility in large volumes during manufacturing, their transition from the laboratory into the market and thus accessibility by end-users. Herein we investigate the applicability of ionogel materials based on a poly(*N*-isopropylacrylamide) gel with the 1-ethyl-3-methylimidazolium ethyl sulfate ionic liquid as fluid flow manipulator in μ PADs using the ionogel as a negative passive pump to control the flow direction in the device. A big challenge undertaken by this contribution is the integration of the ionogel materials into the μ PADs. Finally, the characterisation and the performance of the ionogel as a negative passive pump is demonstrated.

© 2016 Published by Elsevier Ltd.

1. Introduction

Ionic liquids (ILs) are drawing an incredible amount of attention both from academics and the industry due to their environment-friendly properties, and particularly their potential in green chemistry. The rapid growing number of publications and patents can be considered proof of the large amount of research and investment in this area and their potential applicability has been revealed by some inspiring results [1,2]. ILs are salts, completely composed of ions with melting temperatures below 100 °C, a result of their low-charge density and low symmetry ions [1,3–5]. ILs are categorised as “green” solvents thanks to their unique properties, such as negligible vapour pressure, large range of temperatures at liquid stage [4], conventional non-flammability, non-volatility, and their outstanding solvation potential [2,6–10]. Besides, due to their ionic character, most aprotic ILs display high thermal stability with decomposition temperatures around 300–500 °C, high chemical stabilities (extremely redox ro-

bustness), high ionic conductivity, and high solvation ability for organic, inorganic and organometallic compounds with improved selectivity [1–3,11–14]. They are generally described as “designer solvents” and their potential is further extended due to the fact that their physical and chemical properties (such as their thermophysical properties, biodegradation ability or toxicological features, as well as their hydrophobicity and solution behaviours) may be delicately tuned by varying both the cation and the anion [1,3,15–19]. Moreover, their tunable properties are enabling rapid advances in devices and processes for the production, storage and efficient use of energy [1,20].

However, for material applications, the main requirement is immobilising ILs in solid devices while keeping their specific properties, which is highly challenging [21]. Ionogels form a new class of hybrid materials that preserve the main properties of the ILs (liquid-like dynamics and ion mobility) but in a solid or gel like structure, while allowing easy shaping and thus, increasing considerably the potential use of ILs in key areas such as energy, environment and analysis [21,22]. In the case of ionogels, a further dimension is achieved: the ability of keeping the ILs, and their properties, in a solid support, which can be referred to as “flexibility space” [21]. Additionally, the properties of the final ionogel are different from the

* Corresponding author at: Analytical Microsystems & Materials for Lab-on-a-Chip (AMMa-LOAC) Group, Microfluidics Cluster UPV/EHU, Analytical Chemistry Department, University of the Basque Country UPV/EHU, Vitoria-Gasteiz, Spain.
Email address: fernando.benito@ehu.eus (F. Benito-Lopez)

simple combination of each pure component. Ionogels offer a way to further use ionic liquids in technological applications [22]. The combination of gels, with diversified applications of ionic liquids, enables the design of a thrilling combination of functional tailored materials, allowing materials to be custom designed for a wide range of applications such as sustainable chemistry, energy, electronics, medicine, food or cosmetics, among others [22].

“Lab-on-a-Chip” (LOC) or “micro-Total Analysis Systems” (μ TAS) have the greatest potential for integrating multiple functional elements into a small device to produce truly sample-in/answer-out systems [23]. The design, fabrication, flow control, analysis and connection techniques are under continuous development improving among others, the throughput and the automation while at the same time leading to reduced costs [24]. However, the development of fully integrated microfluidic devices is still facing some significant obstacles, including the lack of robust fundamental building blocks for fluid control, the miniaturisation or elimination of external fluidic control elements [23,25]. The control and movement of flows in microchannels comes from microvalves and micropumps. In the case of active valves and pumps, the actuation depends on external power supplies and they require relatively complex procedures for integration into the microfluidic devices which pose a drawback for the device. On the other hand, passive valves/pumps have recently received an overwhelming amount of interest since they do not need any external actuation components and are easy to fabricate [24]. They can be regarded as a response to the need of simple and effective fluid control elements for building low cost and sophisticated lab-on-a-chip devices. These valves are essentially fabricated from stimuli responsive polymer gels [24]. Gels consisting of either physical or chemical cross-links can undergo controlled and reversible shape changes in response to an applied field [26]. In other words, they demonstrate substantial and reversible changes in their equilibrium degree of swelling in response to weak changes in their surroundings (solvent composition, temperature, pH, and supply of electric field, light, etc.) [27–30]. They are referred to, as smart materials, since they are able to perform functions though an external stimulus without the need of any human input, demonstrating potential for “smart” applications, including biomedical devices, drug delivery carriers, scaffolds for tissue engineering, filters and membranes for selective diffusion, sensors for on-line process monitoring and artificial muscles among others [28,31].

In particular ionogels can also be used as stimuli responsive gels. They have many advantages over conventional materials since their robustness, acid/base character, viscosity and other critical operational characteristics can be finely modified through the tailoring of chemical and physical properties of the ILs [24]. The characteristics of the ionogels can be tuned by simply changing the IL and so the actuation behaviour when used as microvalves in microfluidic devices can be more precisely controlled [24,32]. For instance, two interesting approaches that we took in order to control fluid movement in microfluidic devices, were the use of photo-responsive ionogels controlled by light [33] and the use of reversible thermoresponsive ionogel [34].

Although there have been significant developments and some very promising ones in the microfluidics field, still, the amount of commercial products based on microfluidics has, with few exceptions, remained low, due to the critical need of a large variety of costly high performance components (mixers, actuators, reactors, separators, valves and pumps etc.) for fluid control and transport in the devices. The increase of the cost of the devices resulted in the decrease of the market possibilities [35]. Therefore, “Lab on a paper” is being developed to provide an answer to deliver simple, cheap and autonomous devices which are easily manageable by the end-users [36]. These de-

vices have the full potential of classical microfluidics but with a well-focused commercialisation path [37]. Paper is receiving a great amount of attention as a promising substrate material for microfluidic devices not only due to its extremely low cost and ubiquity but also due to its mechanical properties, comprising flexibility, lightness, and low thickness [36]. In particular, μ PADs are a relatively new group of analytical tools, capable of analysing complex biochemical samples, within one analytical run, where fluidic manipulations, like transportation, sorting, mixing or separation are available [35,38].

Thanks to the capillary forces of paper, there is no requirement for external pumps to provide fluid transport inside the paper unlike traditional microfluidic platforms [35]. However this advantage also generates a drawback; the isotropic wicking behaviour of paper and the fluid transportation caused by any exposed surface area prevent the accurate control of the fluid transport on paper materials, making it highly challenging and complicated [39,40]. Lack of fluid control on paper is at this moment the main dragging force for researchers when looking for new capabilities of μ PADs.

In our previous work [35], we offered a solution by presenting a new concept for fluid flow manipulation in μ PADs by introducing two different ionogel materials as passive pumps which were drop-casted at the inlets where the analytes are introduced into the device. It was demonstrated that ionogels highly affected the fluid flow by delaying the flow from the inlet. They revealed two distinctive liquid flow profiles due to their different physical and chemical properties and thus water holding capacities.

In this study, we extend our investigations and introduce another new concept for fluid flow manipulation in μ PADs. Here, we use the ionogel materials as negative passive pumps at the outlet of the μ PADs. The ionogel is able to continuously drive fluids through the μ PAD through the swelling effect, and so, to control the flow direction and flow volume that reach the outlet. In order to generate a useful, reproducible and operative device we investigated a new method for the integration of the ionogel materials into the μ PADs. Finally, the characterisation and the performance of the ionogel as negative passive pump were carried out.

2. Experimental

2.1. Reagents and materials

Whatman Filter paper Grade 1, wax printer XEROX ColourQube 8580 and a hot plate (Labnet International Inc., USA) were provided in order to fabricate the μ PADs. The design of the devices was carried out with the software application AutoCAD™.

For the synthesis of the ionogels, *N*-isopropylacrylamide, *N,N*'-methylene-bis(acrylamide), 2,2-Dimethoxy-2-phenylacetophenone photoinitiator and 1-ethyl-3-methylimidazolium ethyl sulfate were purchased from Sigma-Aldrich, Spain. For gasket fabrication, cyclic olefin copolymer (COP) was provided by Zeonex/Zeonor, Germany and the pressure sensitive adhesive layer (PSA) was gently provided by Adhesive Research, Ireland.

NaOH solution, and phenolphthalein, which are used for the observation of the colour change (pH) on the μ PAD were provided by Sigma-Aldrich, Spain. For visual observation, blue food dye (McCormick, Sabadell, Spain) was used: 5 mL of water with 100 μ L of food dye (high concentration).

2.2. Fabrication of the μ PADs

The μ PADs were fabricated using the wax printing method with standard laboratory filter paper. Firstly, the desired shape of the microfluidic was drawn in AutoCAD and then printed on one side of the

paper. The final dimension of the microfluidic structure, borders and flow channels, are defined only when the wax is absorbed through the full thickness of the filter paper using the hot plate at the desired temperature. The best performance of the devices was obtained by heating the wax printed papers at 125 °C for 6 min.

2.3. Synthesis and integration of the ionogel

The ionogel used for fluid manipulation was obtained by mixing and heating *N*-isopropylacrylamide, *N,N'*-methylene-bis(acrylamide) and a photoinitiator (2,2-Dimethoxy-2-phenylacetophenone) dissolved in 1 mL of 1-ethyl-3-methylimidazolium ethyl sulfate ionic liquid, at 80 °C for 30 min following the same protocol previously described by ourselves [35]. The chemical structure of the ionogel and its position in the μ PADs are illustrated in Fig. 1.

In order to define the shape of the ionogel on the paper device, a COP/PSA gasket was fabricated and adhered to the paper establishing the border of the gel during UV photopolymerisation. The gaskets have a square shape with dimensions of 20 × 20 mm and have a circle inside with a radius of 6 mm.

During the characterisation experiments 30 μ L, 60 μ L and 90 μ L of the ionogel solution were drop-casted and instantly photopolymerised for 6, 12 and 16 min respectively, under 1600 mW cm⁻² in three different circular outlets of the μ PAD using the polymer gaskets. During the proof of concept experiments, 50 μ L of the ionogel solution was drop-casted in the outlet of the μ PAD, using the gasket, and rapidly UV-photopolymerised for 10 min at 1600 mW cm⁻², see Fig. 2.

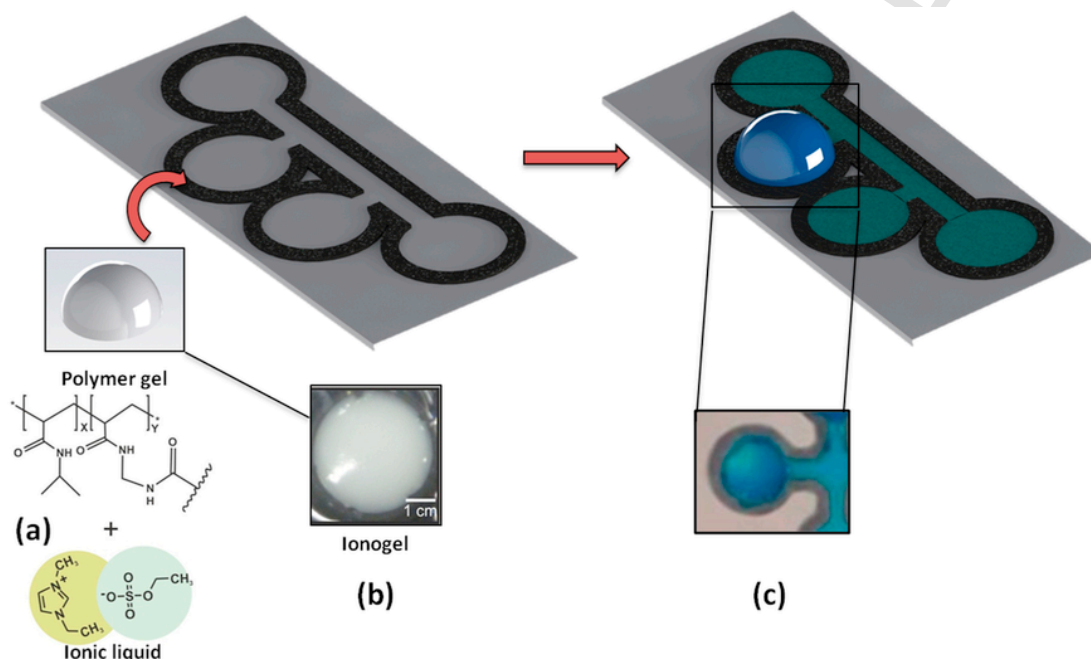


Fig. 1. Scheme of the μ PAD before and after ionogel integration. (A) Chemical structures of the components of the ionogel: polymer gel and 1-ethyl-3-methylimidazolium ionic liquid. (B): picture of the photopolymerised ionogel. (C) Picture of the hydrated ionogel using a blue dye water solution.

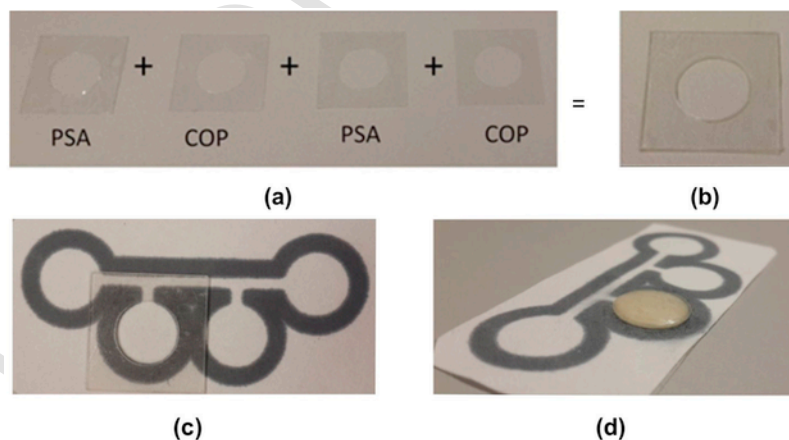


Fig. 2. (a) COP and PSA layers and position to fabricate de gasket, (b) picture of the finalised gasket; (c) μ PAD with adhered polymer gasket ready for the addition of the ionogel solution and subsequent UV photopolymerisation of the ionogel; (d) μ PAD with a defined shaped ionogel after photopolymerisation and removal of the gasket.

In order to remove any unpolymerised material and excess of ionic liquid, the μ PADs with ionogel were washed with deionised water (DI) for 2 min 7 times and let to dry at room temperature for 24 h.

2.4. Measurement protocols

During the characterisation experiments, 50 μ L of blue dye (maximum volume that the inlet can hold without getting overloaded) was dropped in the middle inlet of a μ PAD containing three outlets with 30 μ L, 60 μ L, 90 μ L of photopolymerised ionogel solution and an outlet with no ionogel. This protocol was repeated 10 times to reach a total volume of 500 μ L of blue dye solution in the μ PAD. The fluid flow was recorded with a Samsung Galaxy Note3 camera. Photos of the fluid behaviour of the μ PAD, at different times, were extracted from a video and the volumes of the fluid absorbed by each ionogel were measured with a sensitive digital weight balance (Sartorius, Germany), after being removed from the μ PAD using a Stanley knife (these values include the weight of the paper below the ionogel).

During the proof of concept experiments, two type of straight channel μ PADs having two perpendicular channels, two inlets and two outlets were used; one with no ionogel and another with the photopolymerised ionogel in one of the outlets. An equal volume (180 μ L) of 1.2×10^{-2} M NaOH solution (pH = 12) and 1.2×10^{-2} M phenolphthalein solution (which has a fuchsia colour between pH = 10 and 13) were dropped onto the left and right inlets on both types of μ PAD, respectively, simultaneously. The fluid flow behaviour was recorded with a Samsung Galaxy Note3 camera and the photos of their performance at different times were extracted from the video.

2.5. Interferometry and AFM measurement protocol

Interferometric images were taken with a Bruker contour GT optical microscope. The microscope has a fully automatic turret with X, Y and Z movable stages. The droplets were imaged with a 5 X objective with a 0.55 X zoom lens. The ionogel was imaged at different times during 60 min. A JPK NanoWizard atomic force microscope in intermittent contact mode using a silicon tip ($r < 10$ nm; aspect ratio <6: 1) with a force constant of 40 N m^{-1} and a resonant frequency of approximately 300 kHz was employed to study the topography of the tested material.

In order to study the topography of the ionogel in the drying and swollen states, 20 μ L of the ionogel were photopolymerised, washed with water and dried under vacuum overnight onto a silicon wafer before measurements. The ionogel was rehydrated with 10 μ L of water to study its swollen state.

2.6. Electrochemistry measurement protocol

Regarding the Cyclic voltammetry (CV) measurements, an electrochemical cell consisting of two Au interdigitated electrodes (deposited onto oxidised silicon substrate by RF magnetron sputtering according to literature) was used [41]. The cyclic voltammetry experiments were monitored with the Autolab electrochemical working station PGSTAT 302N using the Nova 1.9 software version (Eco Chemie). All cyclic voltammetry assays were performed under the same conditions using MilliQ water at room temperature. The measurements were carried out in a range between -3 V and 3 V , with a scan rate of 0.1 V/s .

3. Results

3.1. Fabrication of the μ PADs

The wax printing method for μ PAD fabrication is based on patterning hydrophobic barriers of wax in hydrophilic paper using a commercially available printer and a hot plate [42]. The fabrication process consisted of two core operations: (i) printing wax patterns on the paper surface with the wax printer and (ii) the penetration of the wax through the paper thickness by wax melting to form a complete hydrophobic barrier which defines the μ PAD [42]. The μ PAD fabrication followed the same protocol. Nevertheless, since the wax spreads through the paper during the heating process, it is necessary to investigate the relation between the heating temperature/heating time and the final dimensions of the μ PAD (width of the channel and width of the wax barriers) in order to have a homogeneous channel dimension for all the fabricated μ PADs. It is obvious that the dimensions of the printed patterns on the paper do not directly translate into the dimensions of the final hydrophobic patterns in the μ PADs. The best performance was obtained with temperatures of $125 \text{ }^\circ\text{C}$, higher temperatures damaged the shape of the printed patterns (wax is too liquefied and flows out of the defined patterns) while lower temperatures generated inhomogeneous transfer of the patterns and different width dimensions on the wax barriers.

We found out that the ideal heating time is that in which the wax barrier's width of the top and back sides of the μ PAD are equal, so that the width of the final microfluidic channel is well defined and equal in width for all the fabricated devices. Fig. 3 shows a set of experiments carried out at $125 \text{ }^\circ\text{C}$ varying exposition time. It can be observed that after 6 min, both, the top and back channel widths are the same. Therefore, this fabrication protocol (temperature and time) was used for all the μ PADs from then on. This homogeneous channel width ensures that the flow profile over the entire μ PAD is the same.

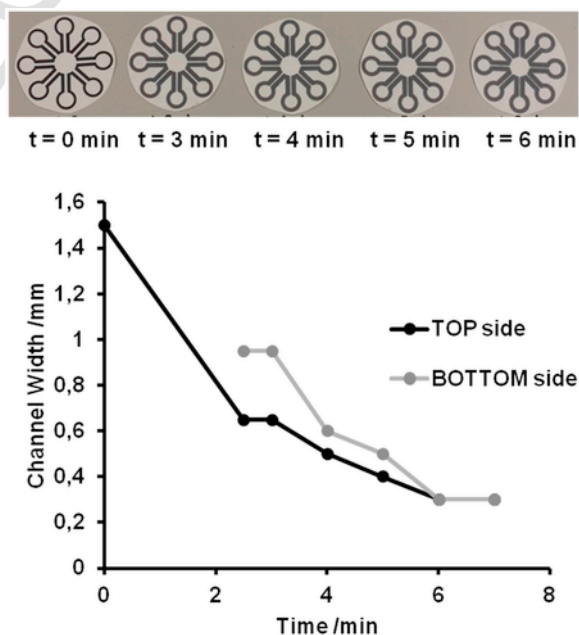


Fig. 3. Pictures of a device at different heating times and graphical representation of the channel width at different heating steps during μ PAD fabrication at $125 \text{ }^\circ\text{C}$ for 8 min (top and bottom sides of the μ PAD). The bottom side is the one in contact with the heater. The best performance was achieved with a channel width $0.30 \pm 0.05 \text{ mm}$ ($n = 3$) at 6 min. The standard deviation is in the range of $\pm 0.03 \text{ mm}$ for all plotted measurements.

The channel width of the μ PADs were measured (with a ruler) to be $0.30 \text{ mm} \pm 0.05 \text{ mm}$ ($n = 3$).

3.2. Integration of the ionogel into the μ PAD

In our previous publication [35] the integration of the ionogel, drop-casting and subsequent photopolymerisation, was carried out using the wax barriers as reservoirs to contain the ionogel solution during the photopolymerisation process. This protocol although effective, was not reproducible from device to device since it was a manual process. Moreover, it limited the volume of the ionogel that could be immobilised, since it was necessary to stop the gel from spreading out of the wax barriers and through the channels. Another drawback was that the ionogel did not have a homogeneous shape for all the devices.

In this study, we developed a new technique, using a COP/PSA gasket, to accommodate the ionogel solution on top of the μ PAD, to generate a homogeneous ionogel shape for all the devices after photopolymerisation and to extend the volume of the ionogel when integrated into the device.

The gasket was pasted to the paper through one of the PSA layers; this ensures that the gasket can be removed after photopolymerisation without peeling off the ionogel. The ionogel solution was photopolymerised, as soon as it was drop-casted onto the gasket. Using rapid photopolymerisation protocols, the spreading of the ionogel solution through the whole paper thickness was minimised, see SEM pictures in publication 35 for clarification, and the “sponge” structure of the ionogel, with the defined shape and borders, was generated on top of the paper, see Fig. 2d.

After photopolymerisation and gasket removal, a short post heating step, $100 \text{ }^\circ\text{C}$ for 2 min, was necessary to regenerate the wax barriers. It was observed that during the drop-casting of the ionogel solution a small amount of wax can be dissolved into the ionogel solution and therefore, generate small, microscopic, paths in the wax barriers for the liquid to break away from the μ PAD. This heating step recovered the tightness of the barriers and did not vary the width channel dimensions ($<5\%$). Finally a washing step was needed to remove all the unpolymerised material and excess of ionic liquid, see experimental section [34,35].

3.3. Fluidic characterisation of the μ PAD

In our previous publication, we demonstrated that the photopolymerised ionogels remained mainly on the surface of the paper and got physically attached mainly to the superficial paper fibers [35]. Therefore during the flow profile experiments, the liquid is expected to naturally flow through the paper fibers of the μ PAD due to the wicking properties of the hydrophilic paper and then, when it reaches the photopolymerised ionogel at the outlet, through the fibers, the negative pumping process of hydration of the ionogel starts taking place.

The ionogel solution volume was varied from 30 to $90 \text{ } \mu\text{L}$ in the μ PAD, and their fabrication performance and fluidic capabilities were investigated. The $30 \text{ } \mu\text{L}$ and $60 \text{ } \mu\text{L}$ ionogel μ PADs were fabricated successfully and the ionogel did not peel off from the paper. However, the 40% of the $90 \text{ } \mu\text{L}$ ionogel μ PADs investigated ($n = 10$), peeled off after photopolymerisation, thus those devices were useless. At volumes higher than $90 \text{ } \mu\text{L}$, the ionogel did not successfully attach to the paper surface because of the high excess of ionogel solution, therefore $90 \text{ } \mu\text{L}$ was determined as the highest volume capable of generating an operative μ PAD for our gasket and channel dimensions.

The fluid behaviour of a μ PAD having different volumes of photopolymerised ionogel in three of its four outlets was investigated. The fluidic behaviour of the three ionogel negative pumps was observed and compared to each other. First, a $50 \text{ } \mu\text{L}$ of coloured (blue) dye solution was injected into the inlet of the device, see Fig. 4a. The liquid coming from the inlet (centre of the μ PAD) dampened the paper, and through the wicking mechanism of the paper it moved through the microfluidic channel to reach the outlets. Then, in the outlets the ionogel absorbed the liquid (hydration process) acting as a negative pump continuously driving the liquid towards the outlets and leaving the inlet dry (Fig. 4b). This process was repeated five times, until the inlet remained wet, ensuring that the three pumps were completely hydrated and so the flow stopped.

Visually it was possible to determine the times when the different negative pumps stopped absorbing liquid, and so, their actuation time was determined. In the outlet with no ionogel the wicking process finalised after $68 \pm 2 \text{ min}$ ($n = 3$) (Fig. 4c). Then, the outlet with $30 \text{ } \mu\text{L}$ ionogel stopped acting as a negative pump after $112 \pm 4 \text{ min}$ ($n = 3$) (Fig. 4d), followed by the $60 \text{ } \mu\text{L}$ ionogel outlet, $141 \pm 4 \text{ min}$ ($n = 3$)

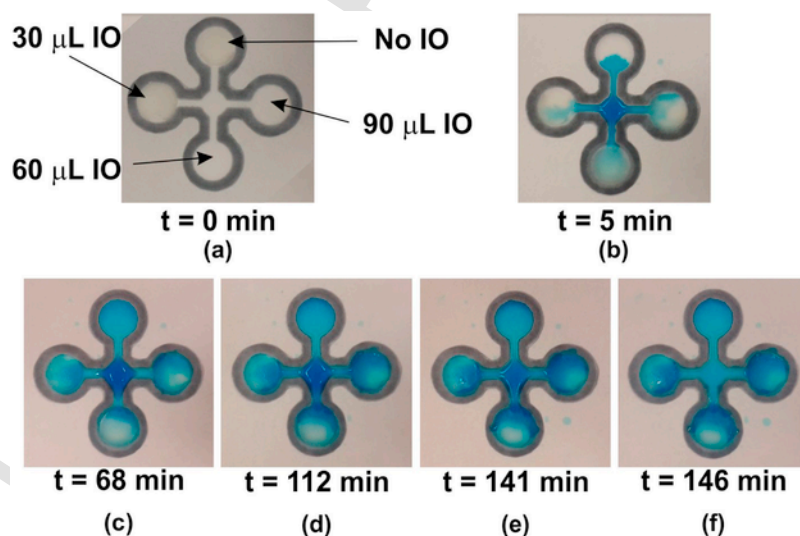


Fig. 4. Actuation time of three different ionogel negative pumps in a single μ PAD (ionogel volumes: 0, 30, 60 and $90 \text{ } \mu\text{L}$).

(Fig. 4e), and finally the outlet with 90 μL ionogel, 146 ± 5 min ($n = 3$) (Fig. 4f). Therefore the actuation time of the negative pumps can be regulated by varying the volume of the ionogel present at the outlet of the μPAD . The higher the volume is, the longer the negative pump actuates.

Fig. 5 shows the water intake capacity of each of the ionogel negative pumps. The volume of the photopolymerised ionogel in the outlet, highly affects the swelling degree of the ionogel and so the capacity of the pump to absorb liquid in the μPAD . For instance, the 90 μL ionogel negative pump was able to absorb 107 ± 10 μL ($n = 3$) of blue dye solution while the bare paper was just able to absorb 17 ± 3 μL ($n = 3$) for the same active area. This opens the possibility of modulating the actuation time of the negative pumps by just varying the volume of the photopolymerised ionogel. Moreover, this behaviour was found to be linear and consistent with small error from device to device. It can be concluded that the wicking property of paper can be highly empowered by the addition of ionogel negative pumps, since gel material has a much higher capacity to absorb water than the bare paper material.

Fig. 6 shows a set of 3D images taken using a Bruker Contour microscope. The images show the morphology and the shape of the ionogel during the hydration process and its evolution over time. The

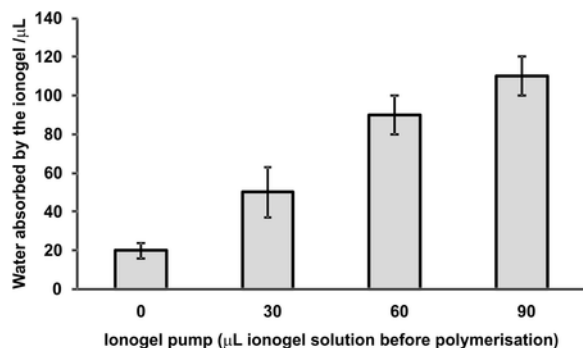


Fig. 5. Water intake capacity of the different ionogel negative pumps ($n = 3$). The error bars represent the standard deviations; which are in the range of ± 10 μL for the 90 μL ionogel pump, ± 8 μL for the 60 μL ionogel pump, ± 11 μL for the 30 μL ionogel pump, and ± 3 μL for the bare paper.

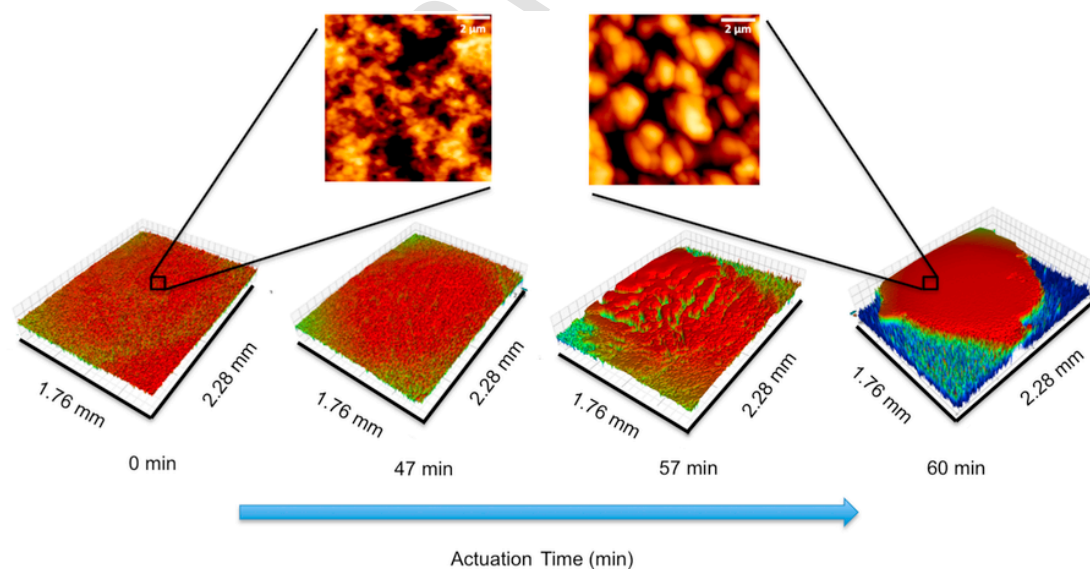


Fig. 6. Top: AFM images of the dehydrated ionogel (left) and hydrated ionogel (right). Bottom: interferometric images at different times during the swelling process of the ionogel.

surface of the ionogel is very porous at the dehydrated stage, with a topography presenting numerous cavities that can be observed in the AFM figures. The surface roughness calculated with the AFM images is 29 ± 6 nm. The dimensions of the pores vary, providing the optimal conditions for water diffusion through the ionogel. When the hydration process starts, the topography of the ionogel varies significantly. The globular shapes of the surface increase in diameter as the ionogel swells. The increase in volume of the ionogel can be observed by comparing the first and the last pictures in Fig. 6. The dimensions of pores are reduced and the surface of the ionogel presents higher irregularities with a roughness of 57 ± 7 nm (see AFM picture at the hydrated stage), growing in volume mainly in the z -axis direction. This could be attributed to the photopolymerisation process, where the restrictions made by the mold leave the ionogel just one degree of freedom in the z -axis direction, which becomes predominant during hydration, as observed by us before [43]. These microscopic observations are in agreement with the behaviour observed by the ionogel negative pump in the μPAD .

Cyclic Voltammetry is a commonly used technique used to obtain information about the interactions between the ionogel and water molecules during the hydration process. Fig. 7a shows a well-defined oxidation and reduction peak of the imidazolium cation with little or no presence of atmospheric moisture. The peaks appear at 1.194 and -1.189 V ($\Delta E = 2.38$ V) and are related to the oxidation and the reduction of the cation of the ionic liquid. The ratio of the peak is almost one, which is indicative of the reversibility of the process [44]. Water was added to the ionogel for hydration, following the same protocol than above (Fig. 7b). It can be observed that the process responsible for the narrowing of the electrochemical window, that is associated to the electrolysis of the absorbed water in the hydration process, does not occur when the voltammograms are scanned from $+3$ to -3 V [45,46]. This is because the Au/Au electrode system needs more extra voltage than Pt/Pt systems for the electrolysis of water, due to the higher activation energy of Au electrodes. [47]

Moreover, there is a considerable shift of both cathodic and anodic peaks, appearing at -0.46 V and 0.34, respectively ($\Delta E = -0.8$ V). Since water in an ionic liquid that leads to a decrease in viscosity, the shift of the reduction and the oxidation peaks can be ascribed to the swollen state of the ionogel. It can be concluded that

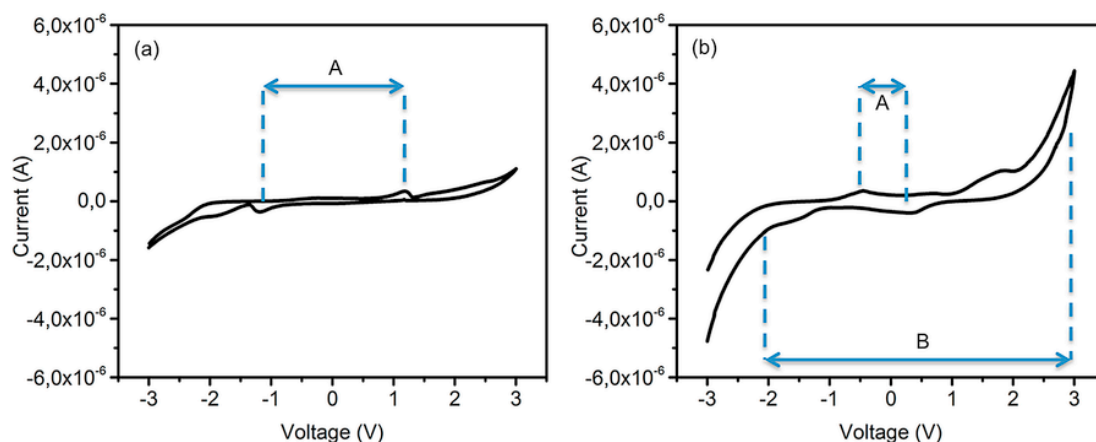


Fig. 7. CV of the ionogel before (a) and after (b) the addition of water. The peaks marked with an A correspond to the redox peaks of the IO after and before the addition of water. The peaks marked with a B correspond to the water hydrolysis peaks.

this state enhances the mass transport of the electrolyte to the electron surface affecting the conductivity.

3.4. Performance of the ionogel negative pumps

As a proof of concept, the fluid flow manipulation capability of the ionogel negative pumps was investigated by comparing the mixing behaviour of two fluids on a μ PAD with no ionogel pumps and a μ PAD with an ionogel pump situated on one outlet. Two different solutions were injected into the μ PAD inlets, simultaneously. On the right side inlet, a solution of NaOH (colourless, pH = 12) was injected, while on the left side inlet, a solution containing phenolphthalein pH indicator (yellow, providing fuchsia colour between pH = 10 and 13) was used. Both solutions flowed towards the centre of the μ PAD thanks to the wicking properties of the paper.

In the case of the μ PAD with no ionogel (Fig. 8a), the mixing point was observed at the middle point of the main channel (Fig. 8a, Picture 3) at $t = 2.5$ min. The wicking property of paper ensures that both solutions flow towards their respective outlets at the same speed until the entire μ PAD gets wet (Fig. 8a, Picture 4), $t = 10$ min. At that point, the wicking forces of paper ended and therefore, there were no additional forces capable of moving the fluid towards a preferred direction. The mixing point was visualised through the formation of a fuchsia colour line at the interface of both solutions due to an abrupt change of pH expressed by the pH indicator (Fig. 8a, Picture 5 and 6) at $t = 30$ min. Then, the pink colour line spread equally in both directions of the μ PAD main channel, by diffusion (Fig. 8a, Picture 8).

In the case of the μ PAD with the ionogel pump (Fig. 8b) a different fluid behaviour was observed. First, the mixing point was found on the left side of the main channel, and not in the middle, as in the bare μ PAD, at $t = 2$ min (Fig. 8b, Picture 3). The location was slightly different than in (a) since the ionogel disturbed the expected flow behaviour of the μ PAD. The hydration process of the ionogel (water intake) was slower in time than the wicking process of the paper. The liquid on the right side of the μ PAD reached the left side of the main channel faster because the outlet-2, on the right μ PAD side, was filled by the ionogel. At the same time the liquid on the left side flowed through the main channel and towards the outlet-1, no ionogel, as in the case of (a). The visualisation of the mixing process, observed through the formation of the fuchsia colour was not so well defined since it happened at the interface of the outlet-1 (Fig. 8b, Picture 4).

Then, when the ionogel started to hydrate, the negative pump commenced its work. It was possible to observe the mixing point of

both fluids. The fuchsia colour (\bullet) was driven to the middle point of the channel first, (Fig. 8b, Picture 5) and then, to the right side of the μ PAD, towards the ionogel (Fig. 8b, Picture 6).

When the ionogel was fully hydrated, it acted as a positive pump releasing water from its matrix and wetting the main channel. This process occurred since the main channel got dry over time (55 min experiment at ambient conditions). The liquid coming from the ionogel pushed away the coloured plug from the ionogel region towards the inlet and the main channel's left side, Fig. 8b, Picture 7. This behaviour would be something impossible to achieve with a conventional paper device. This mechanism can be explained following the hydration behaviour of the ionogel (swelling process, Fig. 6) and considering that the water in-take and release of the ionogel depends on several parameters (1) physical interaction between paper and gel, (in our case, the gel remained mainly on the paper surface and got absorbed in the superficial paper-fibers, allowing the liquid to flow from the paper up to the gel), (2) the type of ionic liquid which highly determines the swelling behaviour of the ionogel (hydrophobicity or hydrophilicity), (3) the porosity level of the gel structure (important for accommodation and release of water), and (4) the geometry of the gel [35].

This behaviour is reproducible. The same flow profile was observed in all the fabricated μ PADs ($n = 6$). The only difference observed among them was the mixing time (120 ± 60 s, $n = 6$), which differed from device to device and can be explained due to the irregular widths obtained during the fabrication process. Another difference was observed in the flow speed generated by the ionogel negative pump (determined by the displacement of the fuchsia mixing point through the main channel), (0.56 ± 0.06 mm min⁻¹). This can be attributed to the small differences in ionogel volume present in the μ PAD, since the drop-casting, photopolymerisation and washing steps of the process are done manually.

Therefore, the flow behaviour on a μ PAD was modulated as desired by introducing the swelling capabilities of the ionogel which acts as negative passive pump. It was proven that it is possible to control the flow direction and even reverse the flow, on a μ PAD, by applying the ionogel negative passive pump in a simple manner.

4. Conclusions

In this contribution a 1-ethyl-3-methylimidazolium ethyl sulfate ionogel was used as a material for the fabrication of negative passive pumps in μ PADs. The integration of a COP/PSA gasket during the

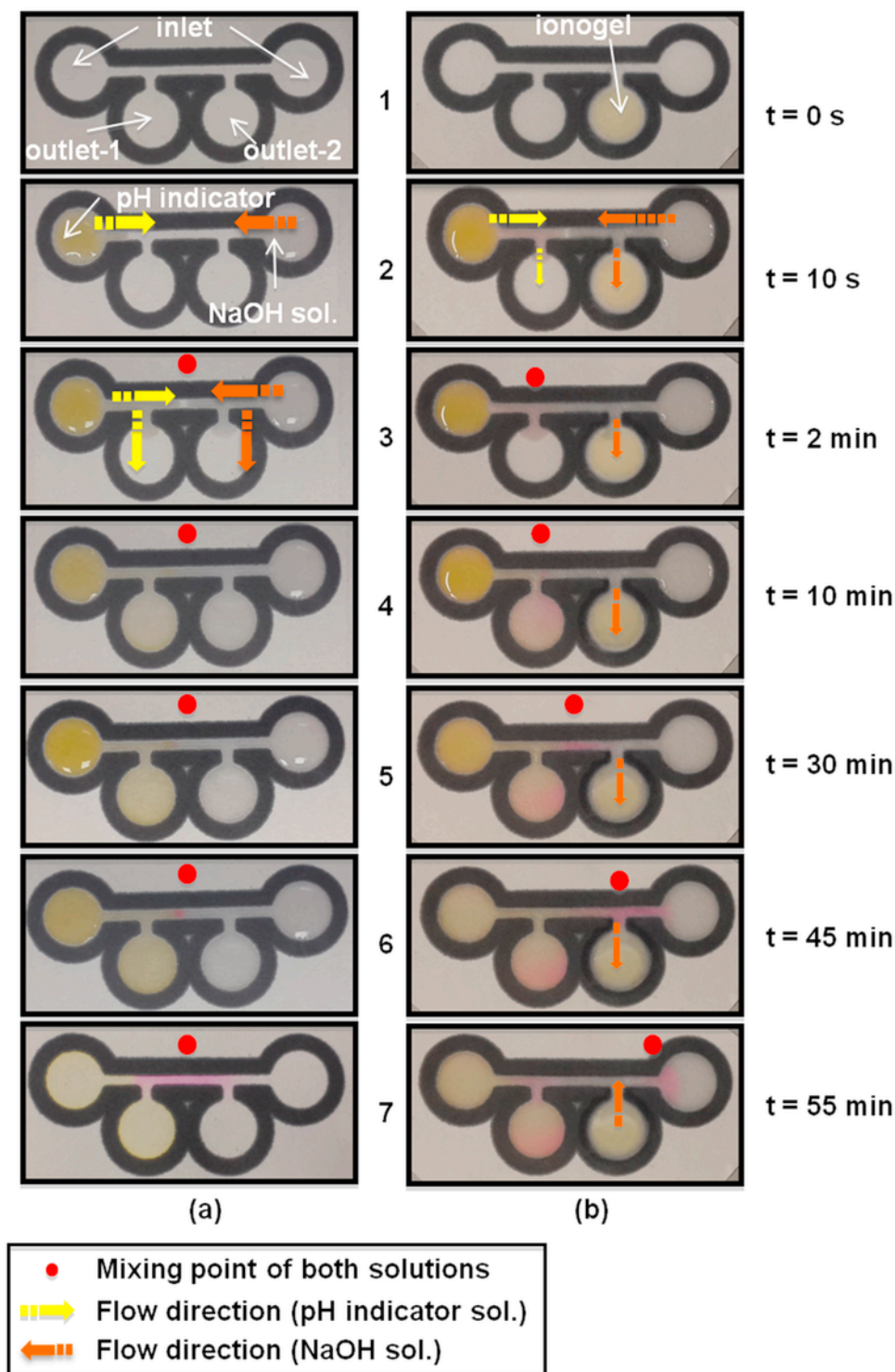


Fig. 8. (a) Pictures showing the fluidic behaviour of a conventional μ PAD over time (wicking forces). The mixing of the two solutions occurs in the middle of the main channel, over the red dot (\bullet). Then, the mixed solution spreads equally in both directions of the μ PAD main channel, by diffusion ($t = 55$ min) (b) Pictures showing the fluidic behaviour of a μ PAD with an ionogel negative passive pump. Arrows show the directions of the flows (yellow: indicator solution) and (orange: basic solution); the red dot (\bullet) shows the mixing point of both solutions and the movement of this point over the μ PAD channel thanks to the negative flow generated by the ionogel pump. (For interpretation of the references to colour in this figure legend, the reader is referred to the web version of this article.)

fabrication protocol allowed the shaping of the ionogel and therefore ensured the integration of different volumes of ionogel in a single μ PAD. Moreover, the gasket allowed the fabrication of homogeneous ionogel shapes which minimised possible manual fabrication errors.

The flow behaviour of the μ PADs can be modulated, redirected even reversed in the presence of an ionogel negative passive pump. This flow control is possible when the wicking process on the paper

has ended and can be extended over time until the hydration of the ionogel has reached completion.

This investigation guaranties the use of ionogel negative passive pumps in μ PADs for many applications in a simple manner without the need of external pumps. It will open the possibility to detect analytes, sequentially and independently from the main μ PAD channel wicking forces, without the need to design complicated 3D configurations.

Acknowledgments

The project was carried out with the support of the Ramón y Cajal programme (Ministerio de Economía y Competitividad). FBL thanks to the European Union's Seventh Framework Programme (FP7) for Research, Technological Development and Demonstration under grant agreement no. 604241 and the Gobierno Vasco, Dpto. Industria, Innovación, Comercio y Turismo under ELKARTEK KK-2015/00088. FBL and TA personally acknowledge Marian M. de Pancorbo for letting them to use her laboratory facilities at UPV/EHU. MCM acknowledges the Basque Government under the Etorrek Program (Grant No. IE14-391) and Dr Seifert for the use of his laboratory facilities. NG-G work was supported by a PhD fellowship from the University of Navarra. Authors also acknowledge Adhesive Research for the donation of the PSA samples.

References

- M. Petkovic, K.R. Seddon, L.P.N. Rebelo, C.S. Pereira, Ionic liquids: a pathway to environmental acceptability, *Chem. Soc. Rev.* 40 (2011) 1383–1403.
- Structures and interactions of ionic liquids 115, in: S. Zhang, J. Wang, X. Lu, Q. Zhou, D.M.P. Mingos (Eds.), *Structures and Bonding*, Springer-Verlag, Berlin-Heidelberg, 2014, pp. 1–197.
- H. Passos, M.G. Freire, J.A.P. Coutinho, Ionic liquid solutions as extractive solvents for value-added compounds from biomass, *Green Chem.* 16 (2014) 4786–4815.
- A. Stark, K.R. Seddon, Ionic liquids, in: A. Seidel (Ed.), *Kirk-Othmer Encyclopedia of Chemical Technology* 26, John Wiley & Sons, Inc., Hoboken, New Jersey, 2007, pp. 836–920.
- K.R. Seddon, Ionic liquids for clean technology, *J. Chem. Technol. Biotechnol.* 68 (1997) 351–356.
- N.V. Plechkova, K.R. Seddon, Applications of ionic liquids in the chemical industry, *Chem. Soc. Rev.* 37 (2008) 123–150.
- C.C. Weber, A.F. Masters, T. Maschmeyer, Structural features of ionic liquids: consequences for material preparation and organic reactivity, *Green Chem.* 15 (2013) 2655–2679.
- M.J. Earle, J.M.S.S. Esperanca, M.A. Gilea, J.N. Canongia-Lopes, L.P.N. Rebelo, J.W. Magee, K.R. Seddon, J.A. Widegren, The distillation and volatility of ionic liquids, *Nature* 439 (2006) 831–834.
- J. Dupont, P.A. Suarez, A.P. Umpierre, Organo-zincate molten salts as immobilising agents for organometallic catalysis, *Catal. Lett.* 73 (2000) 211–213.
- J.S. Wilkes, A short history of ionic liquids—from molten salts to neoteric solvents, *Green Chem.* 4 (2002) 73–80.
- J.M.S.S. Esperanca, J.N. Canongia-Lopes, M. Tariq, L.M.N.B.F. Santos, J.W. Magee, L.P.N. Rebelo, Volatility of aprotic ionic liquids—a review, *J. Chem. Eng. Data* 55 (2010) 3–12.
- R.D. Rogers, K.R. Seddon, Ionic liquids—solvents of the future, *Science* 302 (2003) 792–793.
- F. Guo, S. Zhang, J. Wang, B. Teng, T. Zhang, M. Fan, Synthesis and applications of ionic liquids in clean energy and environment: a review, *Curr. Org. Chem.* 19 (2015) 455–468.
- J. Zhang, A. Bond, Practical considerations associated with voltammetric studies in room temperature ionic liquids, *Analyst* 130 (2005) 1132–1147.
- L.P.N. Rebelo, J.N.C. Lopes, J.M.S.S. Esperanca, H.J.R. Guedes, J. Lachwa, V. Najdanovic-Visak, Z.P. Visak, Accounting for the unique, doubly dual nature of ionic liquids from a molecular thermodynamic and modeling standpoint, *Acc. Chem. Res.* 40 (2007) 1114–1121.
- T. Welton, Room temperature ionic liquids: solvents for synthesis and catalysis, *Chem. Rev.* 99 (1999) 2071–2083.
- R.D. Rogers, K.R. Seddon, Ionic liquids 11 IB: fundamentals, progress, challenges, and opportunities, In: *American Chemical Society Symposium Series*, Washington D.C., 2005.
- J. Ranke, S. Stolte, R. Stoermann, J. Arning, B. Jastorff, Design of sustainable chemical products—the example of ionic liquids, *Chem. Rev.* 107 (2007) 2183–2206.
- M. Earle, K. Seddon, Ionic liquids, green solvents for the future, *Pure Appl. Chem.* 72 (2000) 1391–1398.
- J.F. Wishart, Energy applications of ionic liquids, *Energy Environ. Sci.* 2 (2009) 956–961.
- J. Le Bideau, L. Viau, A. Vioux, Ionogels, ionic liquid based hybrid materials, *Chem. Soc. Rev.* 40 (2011) 907–925.
- P.C. Marr, A.C. Marr, Ionic liquid gel materials: applications in green and sustainable chemistry, *Green Chem.* 18 (2016) 105–128.
- C.T. Culbertson, T.G. Mickleburgh, S.A. Stewart-James, K.A. Sellens, M. Pressnall, *Anal. Chem.* 86 (2014) 95–118.
- M. Czugala, B. Ziolkowski, R. Byrne, D. Diamond, F. Benito-Lopez, Materials science: the key to revolutionary breakthroughs in micro-fluidic devices, *Proceedings SPIE, Nano-Opto-Mechanical Systems* 8107 (2011) 81070C.
- R. Byrne, F. Benito-Lopez, D. Diamond, Materials science and the sensor revolution, *Mater. Today* 13 (2010) 16–23.
- S. Ahn, R.M. Kasi, S. Kim, N. Sharma, Y. Zhou, Stimuli-responsive polymer gels, *Soft Matter* 4 (2008) 1151–1157.
- R.R. Yoshida, T. Okano, Stimuli-responsive hydrogels and their application to functional materials, in: M. Ottenbrite, K. Park, T. Okano (Eds.), *Biomedical Applications of Hydrogels Handbook*, Springer, New York, 2010, pp. 19–43.
- A.D. Drozdov, C.-G. Sanporean, J.D. Christiansen, Modeling the effects of temperature and pH on swelling of stimuli-responsive gels, *Eur. Polym. J.* 73 (2015) 278–296.
- M. Irie, Stimuli-responsive Poly(N-isopropyl-acrylamide) photo- and chemicals-induced phases transitions, in: K. Dusek (Ed.), *Responsive Gels: Volume Transitions: II*, Springer-Verlag, Berlin and Heidelberg, 2013, pp. 63–85.
- E.M. White, J. Yatvin, J.B. Grubbs III, J.A. Bilbrey, J. Locklin, Advances in smart materials: stimuli-responsive hydrogel thin films, *J. Polym. Sci. B: Polym. Phys.* 51 (2013) 1084–1099.
- M.A.C. Stuart, W.T.S. Huck, J. Genzer, M. Mueller, C. Ober, M. Stamm, G.B. Sukhorukov, I. Szleifer, V.V. Tsukruk, M. Urban, F. Winnik, S. Zauscher, I. Luzinov, S. Minko, Emerging applications of stimuli-responsive polymer materials, *Nat. Mater.* 9 (2010) 101–113.
- A. Kavanagh, R. Byrne, D. Diamond, K.J. Fraser, Stimuli responsive ionogels for sensing applications—an overview, *Membranes* 2 (2012) 16–39.
- F. Benito-Lopez, R. Byrne, A.M. Raduta, N.E. Vrana, G. McGuinness, D. Diamond, Ionogel-based light-actuated valves for controlling liquid flow in micro-fluidic manifolds, *Lab Chip* 10 (2010) 195–201.
- F. Benito-Lopez, M. Antofana-Diez, V.F. Curto, D. Diamond, V. Castro-Lopez, Modular microfluidic valve structures based on reversible thermoresponsive ionogel actuators, *Lab Chip* 14 (2014) 3530–3538.
- T. Akyazi, J. Saez, J. Elizalde, F. Benito-Lopez, Fluidic flow delay by ionogel passive pumps in microfluidic paper-based analytical devices, *Sens. Actuators B* 233 (2016) 402–408.
- E. Fu, T. Liang, P. Spicar-Mihalic, J. Houghtaling, S. Ramachandran, P. Yager, Two-dimensional paper network format that enables simple multistep assays for use in low-resource settings in the context of malaria antigen detection, *Anal. Chem.* 84 (2012) 4574–4579.
- E. Livak-Dahl, I. Sinn, M. Burns, Microfluidic chemical analysis systems, *Annu. Rev. Chem. Biomol. Eng.* 2 (2011) 325–353.
- P. Lisowski, P.K. Zarzycki, Microfluidic paper-based analytical devices (μ PADs) and micro total analysis systems (μ TAS): development, applications and future trends, *Chromatographia* 76 (2013) 1201–1214.
- C.R. Mace, R.N. Deraney, Manufacturing prototypes for paper-based diagnostic devices, *Microfluid. Nanofluid.* 16 (2014) 801–809.
- A. Boehm, F. Carstens, C. Trieb, S. Schabel, M. Biesalski, Engineering microfluidic papers: effect of fiber source and paper sheet properties on capillary-driven fluid flow, *Microfluid. Nanofluid.* 16 (2014) 789–799.
- L. Rojo, I. Castro-Hurtado, M.C. Morant-Miñana, G.G. Mandayo, E. Castaño, Enhanced features of Li₂CO₃ sputtered thin films induced by thickness and annealing time, *CrystEngComm* 17 (2015) 1597–1602.
- E. Carrilho, A.W. Martinez, G.M. Whitesides, Understanding wax printing: a simple micropatterning process for paper-based microfluidics, *Anal. Chem.* 81 (2009) 7091–7095.
- M. Czugala, C. O'Connell, C. Blin, P. Fischer, K.J. Fraser, F. Benito-Lopez, D. Diamond, Swelling and shrinking behaviour of photoresponsive phosphonium-based ionogel microstructures, *Sens. Actuators B* 194 (2014) 105–113.
- A. Zuzuarregui, M.C. Morant-Miñana, E. Pérez-Lorenzo, G. Martínez de Tejada, S. Arana, M. Mujika, *IEEE Sens. J.* 14 (2014) 270–277.
- U. Schröder, J.D. Wadhawan, R.G. Compton, F. Marken, P.A.Z. Suarez, C.S. Consorti, R.F. de Souza, J. Dupont, Water-induced accelerated ion diffusion: voltammetric studies in 1-methyl-3-[2,6-(S)-dimethylocten-2-yl]imidazolium tetrafluoroborate, 1-butyl-3-methylimidazolium tetrafluoroborate and hexafluorophosphate ionic liquids, *New J. Chem.* 24 (2000) 1009–1015.

- [46] A.M. O'Mahony, D.S. Silvester, L. Aldous, C. Hardacre, R.G. Compton, Effect of water on the electrochemical window and potential limits of room-temperature ionic liquids, *J. Chem. Eng. Data* 53 (2008) 2884–2891.
- [47] J. Rossmeisl, A. Logadottir, J.K. Nørskov, Electrolysis of water on (oxidized) metal surfaces, *Chem. Phys.* 319 (2005) 178–184.

Tugce Akyazi graduated from Istanbul Technical University as a Metallurgical and Materials engineer. Then she made her master of science in Materials Science and Engineering, in Politecnico di Milano with a double degree from Istanbul Technical University. After working in industry, she is doing her PhD in the group of Dr. Fernando Benito-Lopez at the University of Basque Country (Microfluidics Cluster UPV/EHU). Her interests are microfluidic analytical devices and integration of new materials in microfluidic platforms.

Nerea Gil-González studied Chemistry at the University of the Basque Country. She also obtained her Master's degree in New Materials at the University of the Basque Country and the University of Cantabria. She is doing her PhD at CEIT (Sensors and Analog Electronics Unit). Her main interests are electrochemical characterization techniques and thin film devices

Lourdes Basabe-Desmots is an IKERBASQUE Research Professor and the group leader of BIOMICS microfluidics Research Group at the University of the Basque Country (UPV/EHU). Her team is focused on the development of microtechnologies for lab-on-a-chip applications for biology and medicine, comprising areas such as chemistry, micro and nano engineering of surfaces, optical sensing, microfluidics, microsystems for single cell studies and point of care diagnostics. She is co-founder of the Microfluidics Cluster UPV/EHU. Lourdes studied Chemistry at the Universidad Autónoma de Madrid, then she did a PhD at the University of Twente in Supramolecular Chemistry and Nanotechnology. Following she joined the Biomedical Diagnostics Institute in Dublin where after a postdoc in polymer microfluidics she became a team leader on "microtechnologies for platelet biology". In June 2012 she was appointed Research Professor by IKERBASQUE the Basque Foundation of Science in Spain.

Enrique Castaño received his BS degree in physical science from the Complutense University of Madrid and the PhD degree in physical science from the University of Navarra, San Sebastián. He is currently head of the Sensors and Analog Electronics Unit of Ceit Research Center and his research interest is mainly focused on the design and development of microsystems. He has taken part in more than thirty projects, both industrial and research projects, from which three patents have been obtained. He is the author or co-author of more than 60 scientific and technical papers obtaining "Best Poster Awards" in Eurosensors XIX (Barcelona-2005) and Eurosensors XX (Goteborg-2006). He is also lecturer of Physics and Solid State Physics at the School of Engineering of the University of Navarra.

Maria Carmen Morant-Miñana is Postdoctoral Researcher in the Nanoengineering group at CIC nanoGUNE, Spain. She obtained her PhD degree in Pharmacy from the University of València in 2007 and worked as a postdoctoral researcher in the field of Material Science at the University of Konstanz. Before she assumed her current position in October 2015, she has worked in the development of electrochemical sensors for bio and chemical applications based on thin gold films and new advanced materials. She has authored several articles in recent years, mainly in chemistry and material science journals.

Fernando Benito-Lopez studied chemistry at the Universidad Autónoma de Madrid and completed his master studies in the Departments of Inorganic and Analytical Chemistry in 2002. He obtained his PhD at the University of Twente, The Netherlands, in 2007. He carried out his postdoctoral research in the group of Prof. Dermot Diamond at Dublin City University, Dublin, where in 2010, he became Team Leader in polymer microfluidics. In 2012 he moved to CIC nanoGUNE a Research Centre working in Microtechnology in Spain. From 2015 he is Ramón y Cajal Fellow and leader of the Analytical Microsystems & Materials for Lab-on-a-Chip (AMMa-LOAC) Group, Microfluidics Cluster UPV/EHU, at the University of the Basque Country, Spain.